

SARG: THE HIGH RESOLUTION SPECTROGRAPH OF TNG

R. G. GRATTON, A. CAVAZZA, AND R. U. CLAUDI

*Astronomical Observatory of Padova,
vicolo dell'Osservatorio 5, I-35122 Padova, Italy*

G. BONANNO, P. BRUNO, AND R. COSENTINO

*Astrophysical Observatory of Catania,
Viale A. Doria, 6 I-95125 Catania, Italy*

AND

F. FERRETTI

*Laserpoint,
Via G. Galilei, 1 I-20090 Segrate, Milano, Italy*

Abstract. SARG is the white-pupil cross-dispersed echelle spectrograph under construction for the Telescopio Nazionale Galileo (TNG) telescope; commissioning is scheduled for mid-1999. SARG is a high efficiency spectrograph designed for the spectral range $\lambda = 370$ up to 900 nm, and for resolution from $R = 19,000$ up to $R = 144,000$. SARG uses an R4 echelle grating in quasi-Littrow mode; the beam size is 100 mm giving an RS product of $RS = 46,000$ at order centre. Both single object and long slit (up to 30 arcsec) observing modes are possible. A dioptric camera images the cross dispersed spectra onto a mosaic of two 2048×4096 EEV CCDs (pixel size: $13.5 \mu\text{m}$).

1. Introduction

SARG is one of the baseline instruments foreseen for the TNG.

Scientific drivers are observation of a significant sample of planets orbiting around stars; data on the mechanisms of galaxy formation by statistical studies of the absorption lines in QSO spectra and by analysis of the chemical composition of fossil remnants of very early stellar populations; studies of stellar and planetary atmospheres; and the interstellar medium.

SARG will be a permanently on-line and aligned instrument. The spectrograph covers a spectral range from 370 to 900 nm with a peak efficiency of 16% (at 600 nm). The instrument is designed to work with resolution from $R = 19,000$ up to $R = 144,000$. The field depends by the observation mode (8 arcsec for multi-order observations, 30 arcsec for single-order observations, and single object for multi-order with image slicers). Finally the optics error budget is 80% within 1.6 pixels ($\sim 25\mu\text{m}$, 0.25 arcsec projected in the sky).

2. Design

The final design consists in an R4 echelle spectrograph placed on a platform rigidly fixed to the fork arm about 2 m below the spectroscopic Nasmyth focus. SARG is fed through a train of optics mounted on a dedicated position of a slide within the mechanical structure of the TNG Low Dispersion Spectrograph (LDS). The TNG rotator adaptor will not rotate during observations with SARG, so most of its functions (optical derotation, guide, and active optics) had to be duplicated within SARG. The layout of the spectrograph is shown in Figure 1.

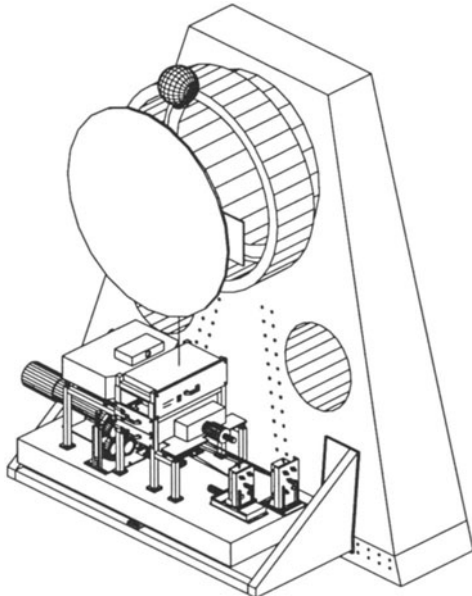


Figure 1. Spectrograph layout.

Following the scheme adopted in various recently built spectrographs (see e.g., the UVES: Dekker *et al.*, 1992), the collimator has a Baranne (1972) white-pupil design, with two off-axis paraboloids. The single blank,

31.6 gr/mm R4 echelle is used in quasi-Littrow configuration. At the center of each order, the slit width-resolution product is $RS = 46,000$ (it ranges from 35,000 to 67,000 at the edges of the order due to anomorphosis). Confocal image slicers (Diego 1994) will be used for observations with resolution $R \geq 76,000$. The whole free spectral range is visualized on the camera for wavelengths shorter than 850 nm. A selection of four grisms mounted on a five-position wheel are used as cross dispersers. SARG has a fully dioptric camera with a focal length of 482.5 mm and a corrected field of 8.5 degrees (radius). The detector is a mosaic of two 2048×4096 (pixel size $13.5 \mu\text{m}$), thinned, back-illuminated CCD chips treated with ion-implantation technology. On this detector, 2 pixels yield a resolution of $R = 144,000$ (at field center).

The main features of SARG mechanics are as follows:

- The feeding unit is located on the Low Dispersion Spectrograph Input Slide while all other components are located on a commercial optical table.
- The SARG optical table is rigidly connected to the TNG fork by a Spectrograph/Telescope Mechanical Interface.
- The Slit Unit carries a number of functions and components distributed in different modular subunits taken in place by a rigid mechanical structure.

In SARG, the ambient temperature is expected to change within rather broad limits with the season (0° to 19°C). In order to avoid deterioration of instrument performances, SARG is located within a thermally insulating enclosure, and functions requiring more frequent maintenance and expected to release significant amount of heat are located outside the enclosure. The temperature inside the enclosure is kept constant at $(20 \pm 0.5)^\circ\text{C}$ by means of a Distributed Active Thermal Control System (DATCS), which may be controlled by software. Also, a heat exchanger prevents the net heat flow through the SARG enclosure to be dissipated in the Nasmyth Room.

3. SARG Performances

Figure 2 displays the V magnitudes for expected S/N with SARG as a function of resolution for a 1 hr exposure (a seeing of 0.8 arcsec is assumed). Some possible targets are listed on the right side of the figure, at approximately their brightest magnitude.

4. SARG Controls

The architecture of the entire system (see Figure 3) is based on a crate VME connected to the other software resources via two links: an FDDI

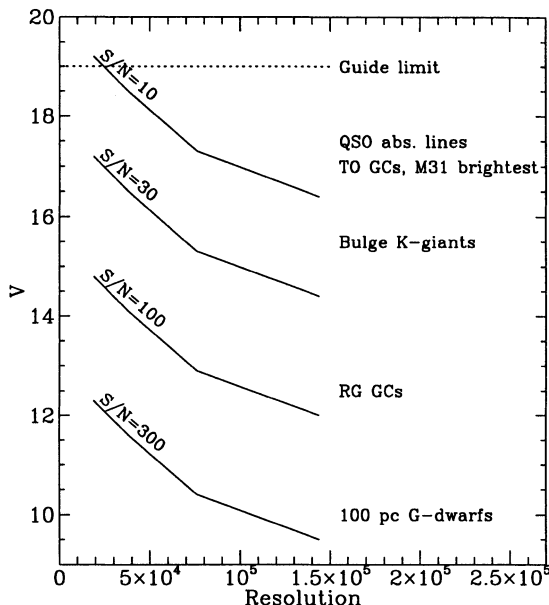


Figure 2. V magnitudes for expected S/N with SARG as a function of resolution for 1 hr exposure (a seeing of 0.8 arcsec is assumed). Some possible targets are listed on the right side of the figure, at approximately their brightest magnitude. Objects fainter than $V=19$ are too faint for telescope guiding using the SARG slit viewer.

(transfer rate 100 Mb/s) to transfer images between CCD controllers and Workstations and an Ethernet (transfer rate of 10 Mb/s) to send/receive commands and telemetry.

High level instrument control functions and user interface will reside on the TNG Instrument Workstation *B*.

An add-on to this architecture is constituted by the IEEE-488 interface that allows one to connect to the system electronic modules that follow the standard protocol HP-IB.

The principal control functions can be divided in different categories:

- Digital IN/OUT: these functions are used for parts that require controls of the on/off switching, telemetry from sensors (temperature, pressure, etc.), and other TNG subsystems
- Motorized remote control functions (rotation of wheels, translation of slides) based on VME boards and on off-the-shelf motor-controllers.
- Exposure meter control function
- CCD Controller Acquisition System, constituted by the scientific and the slit viewer CCD controller

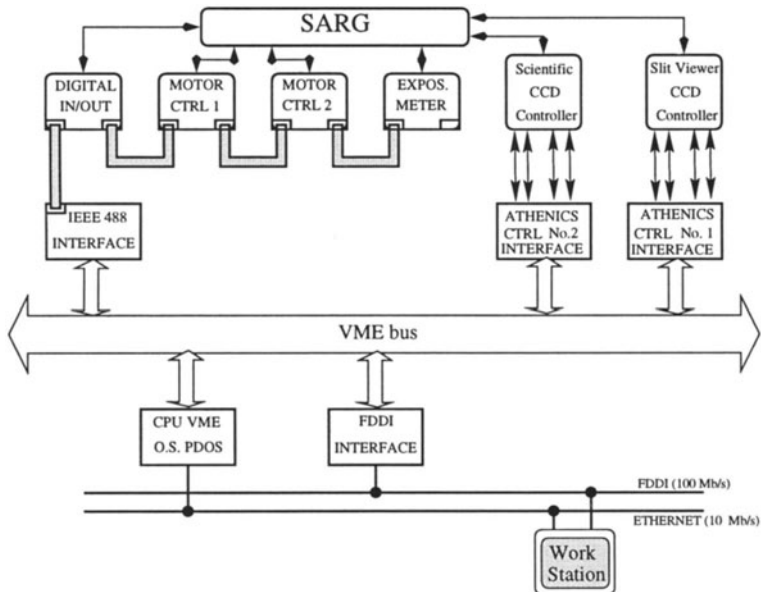


Figure 3. The control architecture of SARG.

5. Schedule

SARG optics design is frozen. The optical components and custom motorized functions will be acquired during 1997. SARG mechanics construction will start within the second half of 1997. The architecture of SARG controls has been defined, and hardware and software will be prepared during 1997. The instrument integration and alignment at the laboratory is foreseen during 1998. Tests at the telescope site and commissioning will be done in the first half of 1999.

References

- Baranne, A., 1972 in *ESO/CERN Conf. on Auxiliary Instrum. for Large Telescope*, eds. S. Laustsen and A. Reiz, Geneva, 227
- Dekker, H., Delabre, B., Hess, G., Kotzlowski, H., 1992, in *Prog. in Telescope and Instrum. Tech.*, ed. M.-H. Ulrich, ESO, Garching, 581
- Diego, F., 1994, in *Instrum. in Astron. VIII*, eds. D .L. Crawford and E. R. Craine, SPIE Proc. **2198**, 525

A REAL-TIME SPECKLE FACILITY FOR THE TELESCOPIO NAZIONALE GALILEO

E. MARCHETTI

*Center for Space Studies and Activities,
University of Padova, Italy*

S. MALLUCCI

Department of Astronomy, University of Bologna, Italy

A. GHEDINA

Department of Astronomy, University of Padova, Italy

J. FARINATO

*Department of Electronics and Informatic Engineering,
University of Padova, Italy*

AND

A. BARUFFOLI, U. MUNARI, AND R. RAGAZZONI

Astronomical Observatory of Padova, Italy

Abstract. Speckle imaging should in principle achieve diffraction-limited images of astronomical objects observed through the blurring effect of the atmospherical turbulence. This paper presents a speckle camera for the Telescopio Nazionale Galileo (TNG), which provides in realtime the auto-correlation of the object shape. The magnification system, the acquisition camera, and the choice of filters are briefly described. The hardware architecture, based upon three 166-MHz CPUs operating within a PCI Bus standard, is also described

1. Introduction

Speckle imaging is a technique (Labeyrie 1970) that allows one to obtain full diffraction-limited performance on images blurred by atmospheric perturbation, provided the focal plane image is analyzed grouping the collected photons into time bins not larger than the mean speckle lifetime (typically of the order of 10 ms at visible wavelengths).

Speckle imaging is, essentially, a post-processing technique on a huge amount of data, which have to be stored on-line. With today's technology, using relatively low-cost hardware, real-time data reduction can be achieved, retrieving only the autocorrelation of the shape of the observed celestial object.

In the adaptive optics system module of the Telescopio Nazionale Galileo (AdOpt@TNG) an independent speckle facility is planned. The TV signal generated by an intensified CCD camera is fed to three different frame grabbers plugged into three industrial, single-board CPUs that digitize, rebin, Fourier transform, and accumulate the obtained Fourier pair of the focal plane image.

After a convenient accumulation time, the three sets of images are co-added in one of the processors and fed to the whole control system. Triggering the frame grabbers, by a dedicated multiplexing device, allows one to relax the time needed to perform real-time processing and to reach a full 25 frames per second autocorrelation function accumulation.

With this low-cost approach, diffraction-limited performances can be achieved even on nearly photon-limited stellar objects.

2. The Magnification System, the Filter Wheel, and the Acquisition Camera

In order to allow full diffraction-limited resolution, the focal plane must be sampled with an appropriate scale by matching the Nyquist criterion in order to have at least four pixels covering the size of the Airy disk at the focus. Because the beam fed into the speckle camera has a focal ratio of F/32 (due to the magnification of a factor 3 of the AdOpt@TNG), the Airy disk, which has an angular dimension of 0.031" at a wavelength of 550 nm, shows a diameter of 18 μm . We want to digitize a subframe with a resolution of 128 \times 128 pixels; in this mode one pixel has a projected dimension on the photocathode of 45 μm , so a magnification of ≈ 10 is required.

Another option of no magnification (1:1) is chosen because we want to use the acquisition camera of the speckle module to control the correction performances of the AdOpt@TNG without using the scientific cameras.

Two lens objectives are selected for the two options: one of 105 mm focal length (1:1 imaging) and one of 35 mm focal length (10 \times magnification). These objectives are mounted in a fixed position on a movable bench. The acquisition camera is a microchannel plate double stage intensified S-25 photocathode coupled to a CCD with an optical fiber bundle. The useful wavelength range is between 360 and 850 nm with a maximum efficiency at 550 nm.

The main control unit could select via digital command the exposure

TABLE 1. The filters adopted in the TNG speckle camera

$\lambda_0 [nm]$	$\Delta\lambda [nm]$	name	notes
475	30	<i>b</i>	colored glass filter [ORIEL 51690]
547	30	<i>y</i>	long-pass [ORIEL 51300] and band pass [ORIEL 51970] filters coupled
550	10	C_2	Swan C_2 absorption band
570	10	$C_2 \text{ cont}$	continuum adjacent to the C_2 band
650	10	ZrO	ZrO absorption band
670	10	TiO	TiO absorption band
660	10	H_α and [NII]	emission lines
580	100	wide-band	this transmission profile is obtained by cutting the camera sensitivity at longer wavelength by means of a short-pass filter [ORIEL 57377, 50%]

time of the acquisition camera as well as the choice of the filters and the magnification desired.

3. Bandwidth Selection

After the objectives, a filter wheel (eight positions) provides the bandwidth selection for different scientific targets. Filter characteristics are shown in Table 1 along with their effective transmittance (see Fig. 1).

The two filters *b* and *y* are intended to match the correspondent Strömgren bands. The *y* filter is composed of a sandwich of (a) a long-pass filter of 50% transmittance at 530 nm, and (b) a band-pass filter with central wavelength of 510 nm and a FWHM bandwidth of 100 nm. The short-pass filter, for general purpose faint objects applications, has a cut-off, at 50%, of 595 nm. The other filters are used for morphological studies of cool stars. The resolution of a large optical telescope is high enough to resolve the stellar disk of nearby giant/supergiant stars (Balega *et al.* 1982, Welter & Worden 1980a, Christou & Worden 1980b), as well as to reveal photospheric asymmetries and surface inhomogeneities (Lynds *et al.* 1976a), and to study the dependence of diameters on wavelength (Bonneau & Labeyrie 1973, Lynds *et al.* 1976ab).

Weigelt *et al.* (1996) show that there is a strong difference in the diameter measured in the TiO absorption band and the diameter measured in the adjacent continuum in the M-type Mira variables. To optimize investigation of cool stars of different chemical abundances, we have selected a set of four filters (marked C_2 , $C_2 \text{ cont}$, TiO, and ZrO in the table) in such a way that the filter for one molecular band is useful for measuring the adjacent continuum in another molecular band.

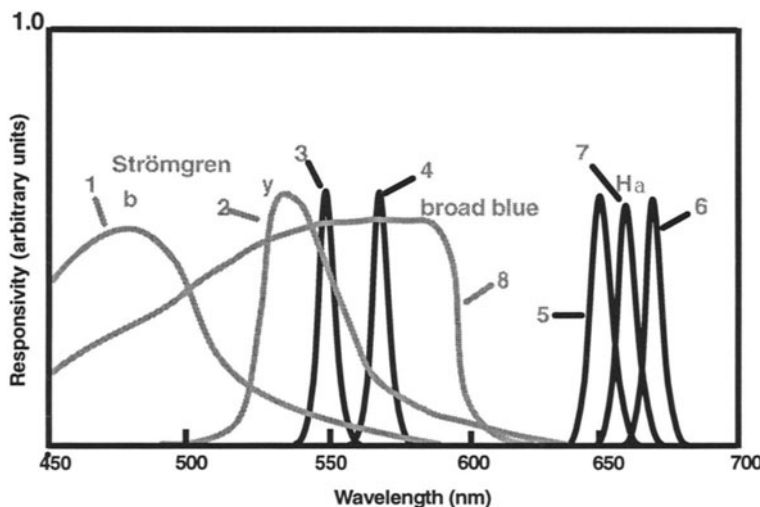


Figure 1. Effective transmittance of the selected filters.

4. Frames Acquisition and Processing

The architecture of the acquisition system and data processing is shown in Fig. 2.

The video signal of the camera (CCIR, a standard B&W at 25 frames/s) is sent to many different devices. One is the vertical synchronism extractor that detects the beginning of each frame and feeds the impulse to a sequencer that sequentially distributes an operating “green light” to the three frame grabbers; when a frame grabber board receives such a signal, a frame digitization occurs. The signal is also sent directly to the three frame grabbers. Optionally, the capability to record on a magnetic tape a movie of the astronomical observed target in order to apply further image processing techniques may be implemented (Liu & Lohmann 1973, Bates & Cady 1980, Knox & Thompson 1974, Weigelt 1977).

Each frame grabber could acquire at 25 frames/second a full 8-bit 754×480 image. Anyway, to allow real-time autocorrelation accumulation at the full frame rate the number and size of images must be conveniently relaxed. As mentioned above, the digitizing boards are triggered in such a way that they acquire just one image out of three: the grabbing sequence for the first board becomes #1,#4,#7..., for the second board #2,#5,#8..., while for the last board it is #3,#6,#9,....

A 128×128 sub-part of a frozen image is stored in the RAM of the respective CPU board via PCI Bus with a transfer rate of 132 Mbytes/second (much higher with respect to the traditional ISA Bus).

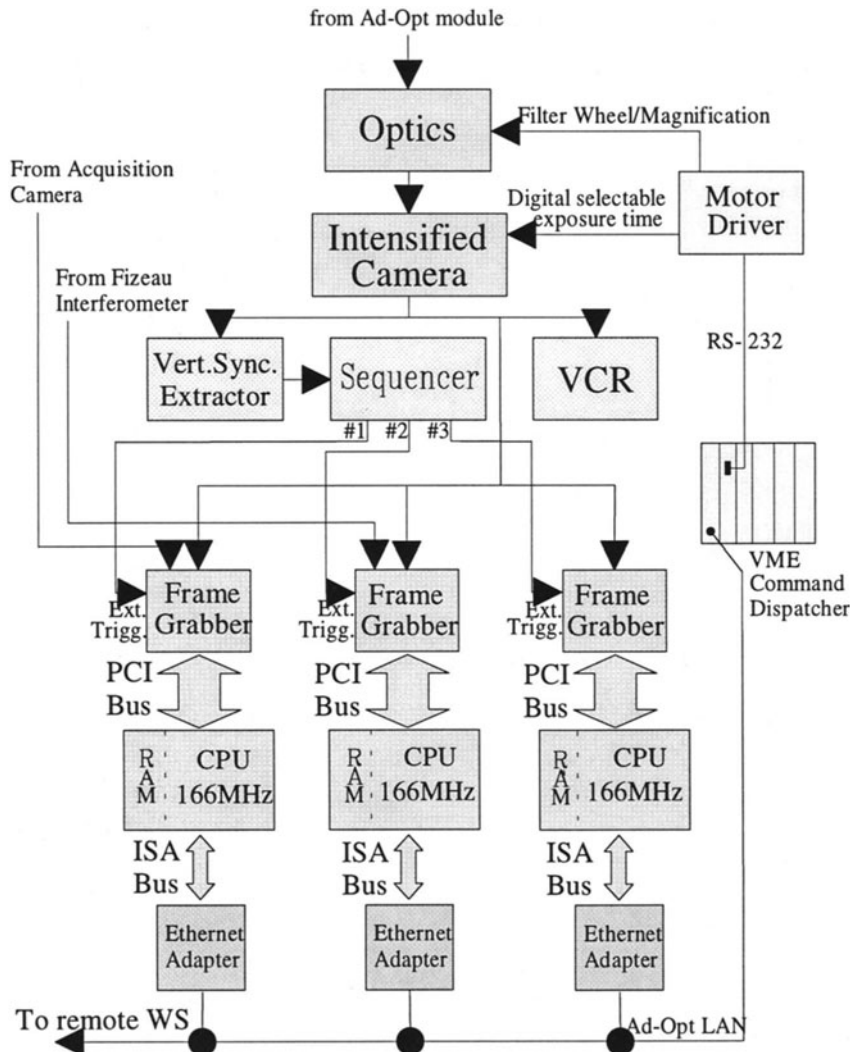


Figure 2. Architecture of the system.

A fast CPU (clocked at 166 MHz) provides the calculation of the power spectrum (namely the squared module of the Fourier transform) of the stored image and the sum between it and the previous bidimensional power spectrum obtained in the same way; the typical benchmark of this CPU to compute a 128×128 spectrum and to store the global sum into the memory amounts to roughly 77 msec. At the end of the process each CPU board transfers its accumulated power spectrum via an Ethernet link to the master PC (one of the three) so that it can be added to the other two.

The whole process has to be performed both for the astronomical target and an unresolved source in order to filter out the power spectrum of the atmospherical turbulence via the experimental measurement of the speckle transfer function (STF).

The autocorrelation function (ACF) of the angular brightness distribution of the astronomical target is retrieved from the inverse Fourier transform by dividing the accumulated data with the STF.

All the functions of the speckle camera are driven by a remote workstation via the AdOpt@TNG local area network.

References

- Balega, I. U., Blazit, A., Bonneau, D., Koechlin, L., Labeyrie, A., Foy, R. (1982) *A&A*, **115**, 253.
Bates, R. H. T., Cady, F. M. (1980) *Opt. Comm.*, **32**, 365.
Bonneau, D., Labeyrie, A. (1973) *ApJ*, **181**, 1L.
Cristou, J., Worden, S. P. (1980b) *AJ*, **85**, 302.
Knox, K. T., Thompson, B. J. (1974) *AJ*, **193**, L45.
Labeyrie, A. (1970) *A&A*, **6**, 85 .
Liu, C. Y. C., Lohmann, A. W. (1973), *Appl. Opt.*, **22**, 4028.
Lynds, C. R., Worden, S. P., Harvey, J. W. (1976a) *ApJ*, **207**, 174.
Weigelt, G. P. (1977) *Opt. Comm.*, **21**, 55.
Weigelt, G. P., Balega, Y., Hofmann, K. H., Scholz, M. (1996) *A&A*, **316**, 21L.
Welter, G. L., Worden, S. P. (1980a) *ApJ*, **242**, 673.
Worden, S. P., Lynds, C. R., Harvey, J. W. (1976b) *JOSA*, **66**, 1243.